

SUSY Electroweakino Searches at the ep Colliders

Georges Azuelos,^{1,2,*} Monica D’Onofrio,^{3,†} Sho Iwamoto,^{4,‡} and Kechen Wang^{5,6,§}

¹*Université de Montréal, Montréal, Québec H3C 3J7, Canada*

²*TRIUMF, Vancouver V6T 2A3, Canada*

³*University of Liverpool, Oliver Lodge Laboratory, P.O. Box 147,
Oxford Street, Liverpool L69 3BX, United Kingdom*

⁴*Physics Department, Technion-Israel Institute of Technology, Haifa 3200003, Israel*

⁵*DESY, Notkestrae 85, D-22607 Hamburg, Germany*

⁶*Center for Future High Energy Physics, Institute of High Energy Physics,
Chinese Academy of Sciences, Beijing, 100049, China*

(Dated: June 11, 2018)

We search for the SUSY dark matter and sleptons at the future electron-proton colliders, LHeC and FCC-eh. We investigate the compressed scenarios where $\tilde{\chi}_1^0$ is bino, $\tilde{\chi}_1^\pm$ and $\tilde{\chi}_2^0$ are wino with almost degenerate masses, and mass difference between $\tilde{\chi}_1^0$ and $\tilde{\chi}_1^\pm$ is 1 GeV. The signal is produced via the process “ $pe^- \rightarrow je^- \tilde{\chi}\tilde{\chi}$ ” with $\tilde{\chi} = \tilde{\chi}_1^0, \tilde{\chi}_1^\pm$ or $\tilde{\chi}_2^0$. We consider the standard model background processes with productions of one or two neutrinos and perform the multivariate analysis at the detector level. When the mass difference between the left-handed slepton \tilde{l} and $\tilde{\chi}_1^\pm, \tilde{\chi}_2^0$, $\Delta M = M_{\tilde{l}} - M_{\tilde{\chi}_1^\pm, \tilde{\chi}_2^0}$, is fixed to be 35 GeV, the $2\text{-}\sigma$ limits on the $\tilde{\chi}_1^\pm, \tilde{\chi}_2^0$ mass are 616 (266) GeV at the FCC-eh (LHeC) with integrated luminosity of $2.5 (1) \text{ ab}^{-1}$ and no systematic uncertainty on the background. To investigate the effects when varying ΔM , we fix $M_{\tilde{\chi}_1^\pm, \tilde{\chi}_2^0}$ to be 400 GeV and find that the significance is maximal when ΔM is around 20 GeV. When sleptons are heavy and decoupled and ignoring the systematic uncertainty on the background, the $2\text{-}\sigma$ limits on the $\tilde{\chi}_1^\pm, \tilde{\chi}_2^0$ mass are 230 GeV at the FCC-eh with integrated luminosity of 2.5 ab^{-1} . We find that 5% systematic uncertainty on the background can affect the limits greatly. We also comment on the effects of the electron beam polarizations. Due to the weak limits of the pp colliders in such compressed scenarios, the searches at the ep collider could be complementary to those at the pp colliders.

I. INTRODUCTION

Supersymmetry (SUSY) is one of the most promising new physics scenarios beyond the Standard Model (SM) and has been searched widely in various production and decay channels at the Large Hadron Collider (LHC). Due to the large production cross sections in strong interactions for the coloured sparticles (gluinos and squarks) at pp colliders, the current LHC experiments at a center-of-mass energy of $\sqrt{s} = 13 \text{ TeV}$ have produced impressive constraints on the coloured particle masses, which are excluded upto to approximately 2 TeV by the ATLAS collaboration with 36.1 fb^{-1} integrated luminosity [1] and by the CMS collaboration with 35.9 fb^{-1} integrated luminosity [2–4].

On the other hand, because of the much lower direct production cross sections for the electroweakinos (neutralinos, charginos and sleptons), so far the LHC constraints on their masses are still limited, which makes the electroweakino searches an increasingly important role in probing the SUSY at future colliders. Previous LHC studies on the searches for the charginos, neutralinos and sleptons during Run 1 at $\sqrt{s} = 7 \text{ TeV}$ and 8 TeV

can be found by the ATLAS Collaboration [5–7] and by the CMS Collaboration [8–11]. Currently, the ATLAS analysis in $2l + 0$ jet final state has placed the limits on the slepton pair $\tilde{l}\tilde{l}$ production and has excluded the slepton masses upto to 500 GeV assuming mass-degenerate \tilde{l}_L and \tilde{l}_R (where \tilde{l} includes all flavors $\tilde{e}, \tilde{\mu}, \tilde{\tau}$) at 13 TeV with 36.1 fb^{-1} luminosity data (cf. Fig. 8(b) of [13]). For charginos and neutralinos, the ATLAS analysis in $2l + \text{jets}$ and $3l$ final states has placed the limits on $\tilde{\chi}_1^\pm \tilde{\chi}_2^0$ production with gauge-boson-mediated decays, and the $\tilde{\chi}_1^\pm, \tilde{\chi}_2^0$ masses have been excluded up to approximately 580 GeV with the same set of data (cf. Fig. 8(d) of [13]).

However, the above limits apply only when assuming a massless $\tilde{\chi}_1^0$ or the mass differences Δm between the \tilde{l} or $\tilde{\chi}_1^\pm/\tilde{\chi}_2^0$ and the lightest supersymmetric particle (LSP) $\tilde{\chi}_1^0$ are large ($\Delta m(\tilde{l}, \tilde{\chi}_1^0) \gtrsim 200 \text{ GeV}$ for \tilde{l} searches and $\Delta m(\tilde{\chi}_1^\pm/\tilde{\chi}_2^0, \tilde{\chi}_1^0) \gtrsim 330 \text{ GeV}$ for $\tilde{\chi}_1^\pm/\tilde{\chi}_2^0$ searches, respectively). When the mass differences are small, which is usually referred to as compressed scenarios or as having compressed mass spectra, the visible products from \tilde{l} and $\tilde{\chi}_1^\pm/\tilde{\chi}_2^0$ decays are very soft. This challenges the analysis and thus the limits are rather weak in such scenario. For example, analysis in Ref. [13] shows null limits when the masses of \tilde{l} and $\tilde{\chi}_1^\pm/\tilde{\chi}_2^0$ above 200 GeV and mass differences $\Delta m(\tilde{l}, \tilde{\chi}_1^0) \lesssim 70 \text{ GeV}$ or $\Delta m(\tilde{\chi}_1^\pm/\tilde{\chi}_2^0, \tilde{\chi}_1^0) \lesssim 100 \text{ GeV}$.

The previous phenomenological studies on the compressed scenarios for the SUSY electroweakino searches can be found in [14–23]. Recently, the ATLAS Collabo-

* georges.azuelos@cern.ch

† Monica.D’Onofrio@cern.ch

‡ sho@physics.technion.ac.il

§ kechen.wang@desy.de

ration perform a search for electroweakinos in final states with two low-momentum leptons and significant missing energy, which targets the neutralino, chargino and slepton decays in the compressed scenarios. Assuming mass-degenerate \tilde{l}_L and \tilde{l}_R (where \tilde{l} includes flavors $\tilde{e}, \tilde{\mu}$), their results at 13 TeV with 36.1 fb^{-1} luminosity exclude the slepton masses up to around 190 GeV with mass splitting $\Delta m(\tilde{l}, \tilde{\chi}_1^0) \sim 1 \text{ GeV}$ (cf. Fig. 11 of [24]). These analyses also exclude the masses of wino $\tilde{\chi}_1^\pm$ and $\tilde{\chi}_2^0$ up to approximately 175 GeV with mass difference $\Delta m(\tilde{\chi}_1^\pm/\tilde{\chi}_2^0, \tilde{\chi}_1^0) \sim 2 \text{ GeV}$ (cf. Fig. 10 of [24]). It is worth noting that such analyses benefit from the softness of the leptons from the slepton and chargino or neutralino decays in the compressed scenarios, and thus the limits are strongest for very small mass splittings. As the mass differences increase, The limits become weak. For example, the 150 GeV sleptons are not excluded by such analyses when $\Delta m(\tilde{l}, \tilde{\chi}_1^0) \gtrsim 10 \text{ GeV}$, while wino chargino and neutralinos with 150 GeV masses are not excluded when $\Delta m(\tilde{\chi}_1^\pm/\tilde{\chi}_2^0, \tilde{\chi}_1^0) \gtrsim 20 \text{ GeV}$. Similar searches in the compressed scenarios with final states of soft leptons has also been reported by the CMS collaboration at $\sqrt{s} = 8 \text{ TeV}$ [10, 25] and at $\sqrt{s} = 13 \text{ TeV}$ [11, 12]. Therefore, the compressed scenarios with heavy electroweakino masses or relatively large mass splittings still eludes the searches at the current pp collider and needs to be investigated at future colliders.

In this article, focusing mainly on the compressed scenarios, we evaluate the sensitivity of ep colliders to discover the SUSY dark matter and sleptons. In Ref. [28], a parton-level analysis on the Higgsino neutralinos and charginos has been performed at the Large Hadron electron Collider (LHeC), which shows that with an integrated luminosity of 1 (3) ab^{-1} , the Higgsino masses could be reached upto to 135 (155) GeV with $2\text{-}\sigma$ significance. Two signal scenarios are considered in this study. In the first scenario, $\tilde{\chi}_1^0$ is bino, $\tilde{\chi}_1^\pm$ and $\tilde{\chi}_2^0$ are wino with nearly degenerate masses and all other SUSY particles are heavy and decoupled, which we called the ‘‘heavy slepton scenario’’. This scenario can be motivated by the dark matter coannihilation arguments [26, 27]. For a bino $\tilde{\chi}_1^0$ dark matter, the annihilation cross-section is usually too low. The wino-dominant $\tilde{\chi}_1^\pm$ and $\tilde{\chi}_2^0$ with masses of order one to tens of GeV larger than a bino $\tilde{\chi}_1^0$ may enhance the coannihilation processes and results in the observed dark matter relic density. In the other ‘‘light slepton’’ scenario, we assume the left-handed slepton \tilde{l}_L and sneutrino $\tilde{\nu}$ are also within the collider access and are slightly heavier than $\tilde{\chi}_1^\pm$ and $\tilde{\chi}_2^0$. The light sleptons can be also motivated by the coannihilation arguments. Furthermore, the measured muon anomalous magnetic moment [29] shows more than $3\text{-}\sigma$ discrepancy from the SM prediction. Since the main SUSY contributions to the muon $g - 2$ are dominated by the neutralino-smuon and chargino-sneutrino loop diagrams, a SUSY mass spectra containing hundreds of GeV neutralinos and sleptons may explain the experimental results of the anomalous magnetic moment of the muon (see [30] for a recent sum-

mary).

In this study, We perform a detector-level simulation at both LHeC and the electron-hadron mode of the Future Circular Collider (FCC-eh). For the electron and proton beam energies at the LHeC and FCC-eh, we consider 60 GeV \times 7 TeV and 60 GeV \times 50 TeV [31–33], respectively. The maximal integrated luminosity for the LHeC is expected to be 1 ab^{-1} , while it can be 2.5 ab^{-1} for the FCC-eh with a 25-year running (1 ab^{-1} per 10 years). Although the center-of-mass energies of 1.3 and 3.5 TeV, respectively, are lower than at pp colliders, the SM QCD backgrounds, which are dominant in the pp colliders, are much smaller at ep colliders since there is no gluon exchange diagrams. Moreover, pile up jets constitute an very important background at pp colliders, especially at high luminosity, but they are essentially negligible at ep colliders. Therefore, the searches at the ep colliders could yield complementary limits on the SUSY electroweakinos especially in the compressed scenarios.

The article is organized as follows. In Sec. II we describe the data simulation, signal and background processes and our search strategy. In Sec. III, we present the results in the light slepton scenario when fixing ΔM and also show the effects when varying ΔM . The results in the heavy slepton scenario is given in Sec. IV. We summarize and conclude in the last Sec. V.

II. SEARCH STRATEGY

For our analysis, the data is simulated by MadGraph5_aMC@NLO [36] as the event generator, followed by Pythia [37] for the parton showering and hadronization, and Delphes [38] for the detector simulation. The detector is assumed to have a cylindrical geometry comprising a central tracker followed by an electromagnetic and a hadronic calorimeter. The forward and backward regions are also covered by a tracker, an electromagnetic and a hadronic calorimeter. The angular acceptance for charged tracks in the pseudorapidity range of $-4.3 < \eta < 4.9$ and the detector performance in terms of momentum and energy resolution of electrons, muons and jets, are based on the LHeC detector design [31, 34]. For our simulation, a modified Pythia version tuned for the ep colliders and the Delphes card files for the LHeC and FCC-eh detector configurations [35] are used.

For the signal production, (suggest to show the diagrams of signal production (perhaps in the introduction).) we consider the Lightest Supersymmetric Particle (LSP) $\tilde{\chi}_1^0$ is bino, while $\tilde{\chi}_1^\pm$ and $\tilde{\chi}_2^0$ are wino with almost degenerate masses. We fix the mass difference between $\tilde{\chi}_1^0$ and $\tilde{\chi}_1^\pm$ to be 1 GeV. The signal is produced via the process ‘‘ $p e^- \rightarrow j e^- \tilde{\chi} \tilde{\chi}$ ’’, where $\tilde{\chi} = \tilde{\chi}_1^0, \tilde{\chi}_1^\pm$ or $\tilde{\chi}_2^0$. Therefore, the final state has 1 jet, 1 electron, large missing energy and undetected very soft particles from $\tilde{\chi}_1^\pm$ or $\tilde{\chi}_2^0$ decays. In our heavy slepton scenario, only $\tilde{\chi}_1^0, \tilde{\chi}_1^\pm$ and $\tilde{\chi}_2^0$ are considered to be light, and all other SUSY particles are heavy and decoupled. Thus, the signal process is de-

scribed by direct production of neutralinos and charginos. In our light slepton scenario, the left-handed slepton \tilde{l}_L and sneutrino $\tilde{\nu}$ are also within the collider access and are assumed to be slightly heavier than $\tilde{\chi}_1^\pm$ and $\tilde{\chi}_2^0$. Besides the direct productions of neutralinos and charginos $p e^- \rightarrow j e^- \tilde{\chi} \tilde{\chi}$, the signal process will also include the direct production of \tilde{l}_L and $\tilde{\nu}$, i.e., $p e^- \rightarrow j \tilde{\chi} \tilde{l}_L, j \tilde{\chi} \tilde{\nu}$, following by the decays of $\tilde{l}_L \rightarrow \tilde{\chi}_{2,1}^0 + e^-$ and $\tilde{\nu} \rightarrow \tilde{\chi}_1^\pm + e^-$. In this article, we consider the masses of the sleptons and sneutrinos such that the sleptons and sneutrinos are produced on its mass shell. When sleptons and sneutrinos are very heavy, they can be off-shell produced, which induces the direct four-body production. (Here, I think we should say that the slepton can be off-shell yielding to direct three-body decay, or it could be on its mass shell.) (For me, so far I am not very clear the off-shell situation. Please check whether the new sentences are correct.)

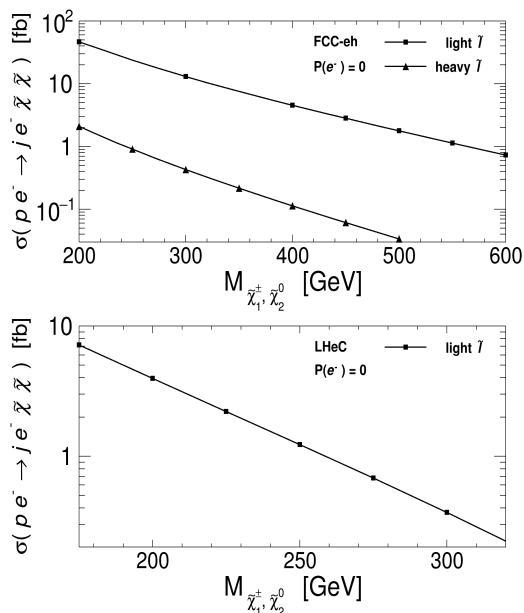


FIG. 1. Production cross sections $\sigma(p e^- \rightarrow j e^- \tilde{\chi} \tilde{\chi})$ in fb for the light slepton and heavy slepton scenarios at the FCC-eh (upper) and for the light slepton scenario at the LHeC (lower) with unpolarized electron beam as varying the masses of $\tilde{\chi}_1^\pm$ and $\tilde{\chi}_2^0$. (Should we remove the 2.5 ab^{-1} curve for LHeC ?)

In Fig. 1, we show the production cross sections in fb for both the light slepton and heavy slepton scenarios at the FCC-eh and for the light slepton scenario at the LHeC with unpolarized electron beam as varying the masses of $\tilde{\chi}_1^\pm$ and $\tilde{\chi}_2^0$. The cross sections are calculated using MadGraph5_aMC@NLO by importing the general MSSM model with the model parameter file generated by the SUSY-HIT package [39].

Due to the presence of large missing energy in the final state, processes with production of neutrinos will contribute to the SM background. We separate the background into two categories: the 2-neutrino process “ $p e^- \rightarrow j e^- \nu \nu$ ” and the 1-neutrino process “ $p e^- \rightarrow$

$j e^- l \nu$ ”, where all flavors of leptons e, ν, τ are included. The 2-neutrino process has the same final state as the signal and is an irreducible background. The 1-neutrino process has a large cross section and will therefore have a non-negligible contribution to the background if one of the two leptons is undetected.

We firstly choose the final states with the following pre-selection cuts:

1. At least 1 jet with $p_T > 20$ GeV;
2. Exactly 1 electron with $p_T > 10$ GeV;
3. No b-jet with $p_T > 20$ GeV;
4. No muon or tau with $p_T > 10$ GeV;
5. Missing energy $\cancel{E}_T > 50$ GeV.

After the pre-selection cuts, the following 17 observables are input to the TMVA package [40] to perform the Multi-Variant Analysis (MVA).

1. global observables:
 - 1.1. the missing energy \cancel{E}_T ;
 - 1.2. the scalar sum of the transverse momentum p_T of all jets H_T .
2. observables for the visible objects:
 - 2.1. p_T and the pseudorapidity η of the first leading jet j_1 and the first leading electron e_1 : $p_T(j_1), \eta(j_1), p_T(e_1), \eta(e_1)$;
 - 2.2. the pseudorapidity difference $\Delta\eta$ and the azimuthal angle difference $\Delta\phi$ between j_1 and e_1 : $\Delta\eta(j_1, e_1), \Delta\phi(j_1, e_1)$;
 - 2.3. the invariant mass M , p_T and η of the system of j_1 and e_1 : $M(j_1 + e_1), p_T(j_1 + e_1), \eta(j_1 + e_1)$.
3. observables between \cancel{E}_T and visible objects:
 - 3.1. $\Delta\phi$ between \cancel{E}_T and j_1, e_1 , or the combination of $j_1 + e_1$: $\Delta\phi(\cancel{E}_T, j_1), \Delta\phi(\cancel{E}_T, e_1), \Delta\phi(\cancel{E}_T, j_1 + e_1)$;
 - 3.2. the transverse mass M_T of the system of \cancel{E}_T and j_1, e_1 or the combination of $j_1 + e_1$: $M_T(\cancel{E}_T, j_1), M_T(\cancel{E}_T, e_1), M_T(\cancel{E}_T, j_1 + e_1)$.

III. RESULTS IN LIGHT SLEPTON SCENARIO

A. Results When Fixing $\Delta M = M_{\tilde{l}} - M_{\tilde{\chi}_1^\pm, \tilde{\chi}_2^0}$

In the light slepton scenario, besides the $\tilde{\chi}_1^0, \tilde{\chi}_1^\pm$ and $\tilde{\chi}_2^0$, the left-handed slepton \tilde{l}_L and the sneutrino $\tilde{\nu}$ are also assumed to be within the collider access. Other SUSY particles are heavy and decoupled. In this subsection, the mass difference between \tilde{l}_L and $\tilde{\chi}_1^\pm$ is fixed to be 35 GeV (i.e., $\Delta M = M_{\tilde{l}} - M_{\tilde{\chi}_1^\pm, \tilde{\chi}_2^0} = 35$ GeV). The $\tan\beta$ value is

fixed to be 30, such that the mass difference between \tilde{l}_L and $\tilde{\nu}$ is around 9 GeV. In such a scenario, regarding to the leptonic decays of \tilde{l}_L and $\tilde{\nu}$, the branching ratios are $\text{BR}(\tilde{l}_L \rightarrow \tilde{\chi}_{2,1}^0 + e^-) \approx 40\%$ and $\text{BR}(\tilde{\nu} \rightarrow \tilde{\chi}_1^\pm + e^-) \approx 60\%$. We derive the discovery sensitivities for such a scenario at both the FCC-eh and LHeC. The benchmark mass for $\tilde{\chi}_1^\pm, \tilde{\chi}_2^0$ are chosen to be 400 GeV and 250 GeV at the FCC-eh and LHeC, respectively.

In Fig. 8, we show the kinematical distributions of some selected input observables for signal $j e^- \tilde{\chi} \tilde{\chi}$ with $M_{\tilde{\chi}_1^\pm, \tilde{\chi}_2^0} = 400$ GeV (black with filled area) in the light slepton scenario, and the SM background of the $j e^- \nu \nu$ (red) and $j e^- l \nu$ (blue) processes after applying the pre-selection cuts at the FCC-eh with the unpolarized electron beam. The similar plots at the LHeC for signal with $M_{\tilde{\chi}_1^\pm, \tilde{\chi}_2^0} = 250$ GeV and SM background processes are presented in the Fig. 9.

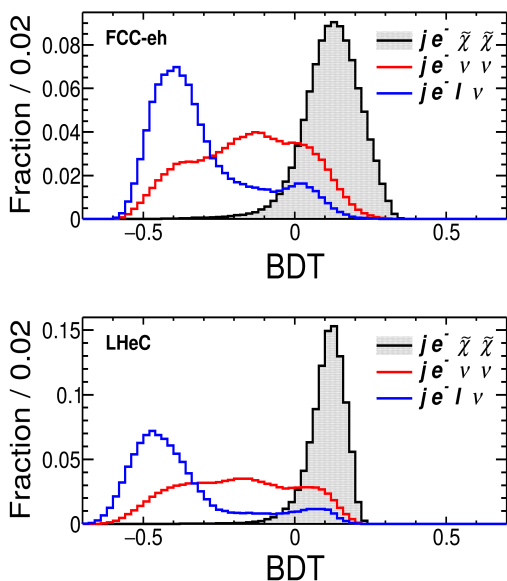


FIG. 2. Distributions of BDT response at the FCC-eh (upper) and the LHeC (lower) with the unpolarized electron beam for signal $j e^- \tilde{\chi} \tilde{\chi}$ (black with filled area) in the light slepton scenario, and for the SM backgrounds of the $j e^- \nu \nu$ (red) and $j e^- l \nu$ (blue) processes after applying the pre-selection cuts. For the signals, $M_{\tilde{\chi}_1^\pm, \tilde{\chi}_2^0}$ is 400 GeV and 250 GeV at the FCC-eh and LHeC, respectively.

The observables are input to the TMVA package and the Boosted Decision Trees (BDT) method is adopted to perform the MVA analysis. In the upper plot of Fig. 2, we show the distributions of BDT response for signal $j e^- \tilde{\chi} \tilde{\chi}$ with $M_{\tilde{\chi}_1^\pm, \tilde{\chi}_2^0} = 400$ GeV (black with filled area) in the light slepton scenario, and for the SM backgrounds of the $j e^- \nu \nu$ (red) and $j e^- l \nu$ (blue) processes after applying the pre-selection cuts at the FCC-eh with the unpolarized electron beam. The lower plot shows the distributions of BDT response at the LHeC for signal with $M_{\tilde{\chi}_1^\pm, \tilde{\chi}_2^0} = 250$ GeV and SM background processes.

In Table I, we show the numbers of events at each cut stage for signal with $M_{\tilde{\chi}_1^\pm, \tilde{\chi}_2^0} = 400$ GeV in the light slepton scenario, and for the SM background processes at the FCC-eh with unpolarized electron beam and an integrated luminosity of 1 ab^{-1} .

For this study, the statistical significance, σ_{stat} , of the potential signal is evaluated as

$$\sigma_{\text{stat}} = \sqrt{2[(N_s + N_b) \ln(1 + \frac{N_s}{N_b}) - N_s]} \quad (1)$$

where N_s (N_b) are the expected number of events for signal (background). Taking into account a systematic uncertainty of σ_b in the evaluation of the number of background events, Eq. (2) will be used to evaluate the significance:

$$\sigma_{\text{stat+syst}} = \left[2 \left((N_s + N_b) \ln \frac{(N_s + N_b)(N_b + \sigma_b^2)}{N_b^2 + (N_s + N_b)\sigma_b^2} - \frac{N_b^2}{\sigma_b^2} \ln \left(1 + \frac{\sigma_b^2 N_s}{N_b(N_b + \sigma_b^2)} \right) \right) \right]^{1/2} \quad (2)$$

The benchmark mass point has $\Delta M = 35$ GeV, which corresponds to the column with $m_{\tilde{\chi}} = 400$ GeV and $m_{\tilde{l}} = 435$ GeV in Table I. The number of signal and background events after applying the pre-selection cuts and the optimized BDT cut are 149 and 686.5, respectively. When considering a systematic uncertainty of 5% on the background (i.e., $\sigma_b = 5\% N_b$), using the Eq. 2, the significance for the benchmark point is 3.28, which is shown in the last row of the Table I.

The cut flow Table II shows the numbers of events at the LHeC with unpolarized electron beam for signal with $M_{\tilde{\chi}_1^\pm, \tilde{\chi}_2^0} = 250$ GeV and for the SM background processes. The numbers corresponds to an integrated luminosity of 1 ab^{-1} . When including 5% systematic uncertainty, the significance of 1.03 can be achieved for this benchmark mass.

Since the kinematical distributions vary with $M_{\tilde{\chi}_1^\pm, \tilde{\chi}_2^0}$, the BDT distributions will also change for different masses. Therefore, We scan the masses and re-optimize the BDT cut for each mass case. In the upper plot of Fig. 3, we present the significance curve relative to the masses of $\tilde{\chi}_1^\pm$ and $\tilde{\chi}_2^0$ for the light slepton scenario at the FCC-eh with unpolarized electron beam and integrated luminosities of 1 ab^{-1} (blue) and 2.5 ab^{-1} (red). For dashed (solid) curve, a systematic uncertainty of 0% (5%) on the background is included. When considering 0% (5%) systematic uncertainty on the background, the 2- σ limits on the $\tilde{\chi}_1^\pm, \tilde{\chi}_2^0$ mass are 567 (451) GeV for 1 ab^{-1} luminosity and 616 (466) GeV for 2.5 ab^{-1} luminosity, while the 5- σ limits are 464 (355) GeV for 1 ab^{-1} luminosity and 517 (367) GeV for 2.5 ab^{-1} luminosity, respectively. Therefore, the systematic uncertainty can affect the limits a lot. In order to enhance the discovery power of SUSY electroweakinos at the future ep colliders, the controlling of the systematic uncertainty is very important.

FCC-eh [1 ab ⁻¹]	Signal						Background	
$m_{\tilde{\chi}} [\text{GeV}]$	400	400	400	400	400	400	$j e^- \nu \nu$	$j e^- l \nu$
$m_{\tilde{l}} [\text{GeV}]$	405	412	420	435	450	465		
initial	4133	4583	4765	4564	4315	4067	1.08×10^6	7.96×10^6
Pre-selection	290	591	2255	3000	2967	2847	3.87×10^5	5.71×10^5
BDT > 0.2257	35.7	-	-	-	-	-	24.8	14.4
BDT > 0.2459	-	30.5	-	-	-	-	17.8	5.1
BDT > 0.2600	-	-	139	-	-	-	132	59.6
BDT > 0.2624	-	-	-	149	-	-	600	86.5
BDT > 0.2597	-	-	-	-	102	-	586	34.9
BDT > 0.2461	-	-	-	-	-	93.3	641	75.4
$\sigma_{\text{stat+syst}}$	4.78	5.23	7.23	3.28	2.47	2.02		

TABLE I. Cut-flow talbe for signal $j e^- \tilde{\chi} \tilde{\chi}$ with $M_{\tilde{\chi}_1^\pm, \tilde{\chi}_2^0} = 400$ GeV in the light slepton scenario, and the SM background processes of $j e^- \nu \nu$ and $j e^- l \nu$. The numbers of events correspond to an integrated luminosity of 1 ab⁻¹ at the FCC-eh with unpolarized electron beam. The significance including 5% systemic uncertainties on the background are presented in the last row.

LHeC [1 ab ⁻¹]	Signal	Background	
$m_{\tilde{\chi}} [\text{GeV}]$	250	$j e^- \nu \nu$	$j e^- l \nu$
$m_{\tilde{l}} [\text{GeV}]$	285		
initial	1231	2.80×10^5	2.01×10^6
Pre-selection	453	6.60×10^4	1.66×10^5
BDT > 0.1717	49.5	486	278
$\sigma_{\text{stat+syst}}$	1.03		

TABLE II. Cut-flow talbe for signal $j e^- \tilde{\chi} \tilde{\chi}$ with $M_{\tilde{\chi}_1^\pm, \tilde{\chi}_2^0} = 250$ GeV in the light slepton scenario, and the SM background processes of $j e^- \nu \nu$ and $j e^- l \nu$. The numbers of events correspond to an integrated luminosity of 1 ab⁻¹ at the LHeC with unpolarized electron beam. The significances including 5% systemic uncertainties on the background are presented in the last row.

The lower plot of Fig. 3 shows the significance curve at the LHeC with unpolarized electron beam and an integrated luminosity of 1 ab⁻¹. With 0% (5%) systematic uncertainty on the background, the limits on the mass are 266 (224) GeV and 227 (187) GeV corresponding to the 2 and 5- σ significances, respectively.

B. Effects When Varying ΔM

When the masses of $\tilde{\chi}_1^\pm$ and $\tilde{\chi}_2^0$ are fixed, different \tilde{l} mass also leads to the changing in the kinematical distributions. To investigate the sensitivities when varying the mass difference ΔM between $\tilde{\chi}_1^\pm$ and \tilde{l} , we fix the $M_{\tilde{\chi}_1^\pm, \tilde{\chi}_2^0} = 400$ GeV and vary the ΔM from 5 GeV to 65 GeV.

The distributions of the BDT response at the FCC-eh corresponding to different ΔM values are shown in Fig. 4. One can see that as ΔM increases, the 2-neutrino background $j e^- \nu \nu$ (red) has larger overlap with the signal $j e^- \tilde{\chi} \tilde{\chi}$ (black with filled area), while when $\Delta M > 35$ GeV the 1-neutrino background $j e^- l \nu$ (blue) also over-

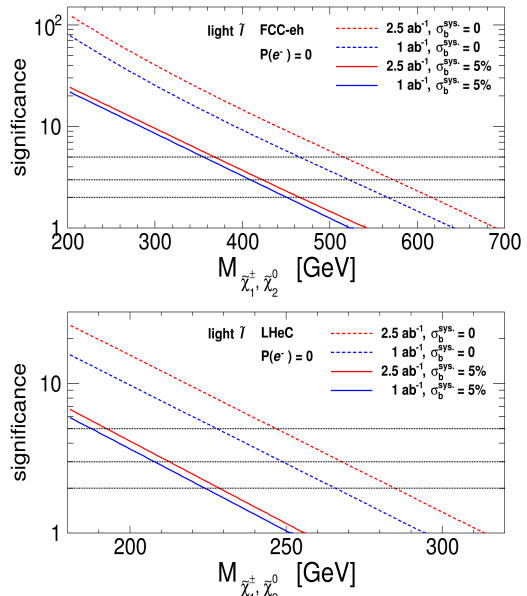


FIG. 3. Significances as varying the masses of $\tilde{\chi}_1^\pm$ and $\tilde{\chi}_2^0$ for the light slepton scenario. Upper plot: at the FCC-eh with unpolarized beams and integrated luminosities of 1 ab⁻¹ and 2.5 ab⁻¹; Lower plot: at the LHeC with unpolarized beams and 1 ab⁻¹ luminosity. For dashed (solid) curve, a systematic uncertainty of 0% (5%) on the background is considered.

laps a lot with the signal. Thus, due to much better separations between the signal and background, it is easier to reject the SM background for small ΔM .

In Table I, we show the numbers of events at the each cut stage for the signals with different ΔM values and background processes. Here, the numbers correspond to FCC-eh with an integrated luminosity of 1 ab⁻¹ and the BDT cut is optimized according to each ΔM value. The significances including 5% systematic uncertainties on the background are presented in the last row.

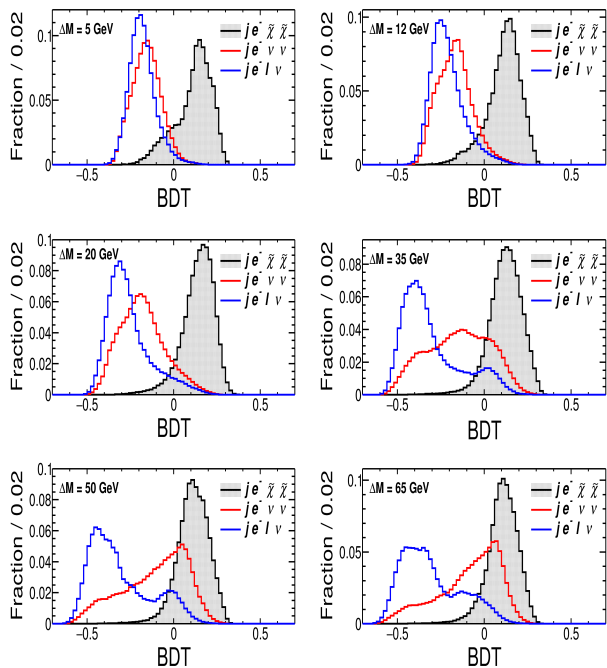


FIG. 4. Distributions of the BDT response when fixing slepton mass $M_{\tilde{\chi}_1^\pm, \tilde{\chi}_2^0} = 400$ GeV and varying the mass difference $\Delta M = M_{\tilde{l}} - M_{\tilde{\chi}_1^\pm, \tilde{\chi}_2^0}$ in the light slepton scenario at the FCC-eh. (Should we remove $\Delta M = 35$ GeV plot since it has been shown in Fig. 2 ?)

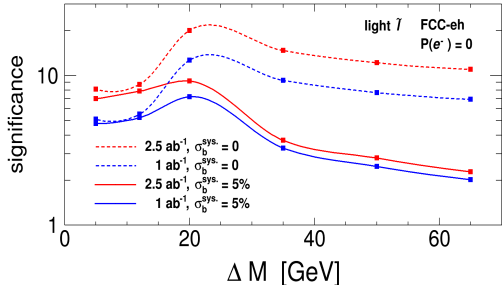


FIG. 5. Significances as varying the mass difference of $\Delta M = M_{\tilde{l}} - M_{\tilde{\chi}_1^\pm, \tilde{\chi}_2^0}$ and $\tilde{\chi}_2^0$ when fixing the slepton mass $M_{\tilde{\chi}_1^\pm, \tilde{\chi}_2^0} = 400$ GeV in the light slepton scenario at the FCC-eh.

The significances with both 5% and 0% systematic uncertainties on the background as varying the mass differences ΔM are also plotted in the Fig. 5. The blue (red) curves corresponds to 1 (2.5) ab^{-1} luminosity, while for the dashed (solid) curve, a 0% (5%) systematic uncertainty on the background is considered. One can see that the $\Delta M = 20$ GeV gives the maximal significances. This is because firstly, as shown in 4, for small ΔM cases, the BDT distributions have better separations between the signal and background, which makes the BDT cut more effectively to reject the SM background. Moreover, when $\Delta M < 20$, the electron from the slepton and sneutrino decays will become too soft to pass the pre-selection cuts

$p_T(e^-) > 10$ GeV, which will reduce the signal number of events a lot. Therefore, with better signal and background separation and relatively large signal number of events after the pre-selection cuts, the maximal significances is achieved when ΔM is around 20 GeV.

It is worth noting that, although the significances for $\Delta M = 12$ and 5 GeV are slightly lower than the that for $\Delta M = 20$ GeV, they are still larger than our benchmark case where $\Delta M = 35$ GeV when 5% systematic uncertainty on background is included. However, when no systematic uncertainty on background is considered, $\Delta M = 35$ GeV gives larger significances compared to $\Delta M = 5$ GeV. This means that if the systematic uncertainty is small, the expected discovery mass reach for very compressed scenarios (for example, $\Delta M \sim 5$ GeV) could be stronger than or at least comparable to our limits obtained for the $\Delta M = 35$ GeV case, while if the systematic uncertainty is large, the mass reach for very compressed scenarios will be much weaker than our limits obtained for the $\Delta M = 35$ GeV case. Therefore, to enhance the discovery power of the very compressed SUSY electroweakino scenarios, the controlling of the systematic uncertainty can be very important.

IV. RESULTS IN HEAVY SLEPTON SCENARIO

In the heavy slepton scenario, only $\tilde{\chi}_1^0$, $\tilde{\chi}_1^\pm$ and $\tilde{\chi}_2^0$ are assumed to be within the collider access and all other SUSY particles are assumed to be heavy and decoupled. Because of the lack of slepton and sneutrino productions, the signal is produced from the direct production of charginos and neutralinos only. Thus, the signal production cross section is much lower in the heavy slepton scenario than that in the light slepton scenario (cf. the upper plot of Fig. 1). In this section, we show our analysis results for the heavy slepton scenario at the FCC-eh.

In Fig. 10, we present the kinematical distributions of some selected input observables at the FCC-eh for signal $j e^- \tilde{\chi} \tilde{\chi}$ with $M_{\tilde{\chi}_1^\pm, \tilde{\chi}_2^0} = 250$ GeV (black with filled area) in the heavy slepton scenario, and the SM background of the $j e^- \nu \nu$ (red) and $j e^- l \nu$ (blue) processes after applying the pre-selection cuts.

The distributions of BDT response at the FCC-eh for signal $j e^- \tilde{\chi} \tilde{\chi}$ with $M_{\tilde{\chi}_1^\pm, \tilde{\chi}_2^0} = 250$ GeV (black with filled area) in the heavy slepton scenario, and the SM background of the $j e^- \nu \nu$ (red) and $j e^- l \nu$ (blue) processes after applying the pre-selection cuts are shown in Fig. 6.

The numbers of events at each cut stage for signal $j e^- \tilde{\chi} \tilde{\chi}$ with $M_{\tilde{\chi}_1^\pm, \tilde{\chi}_2^0} = 250$ GeV in the heavy slepton scenario, and the SM background processes $j e^- \nu \nu$ and $j e^- l \nu$ are presented in Table III. The numbers correspond to an integrated luminosity of 1 ab^{-1} at the FCC-eh with unpolarized electron beam. The significance including 5% systematic uncertainty on the background are presented in the last row.

In Fig. 7, we show the significance plot as varying the

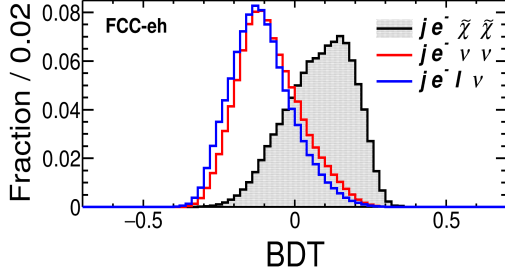


FIG. 6. Distributions of BDT response at the FCC-eh for signal $j e^- \tilde{\chi} \tilde{\chi}$ with $M_{\tilde{\chi}_1^\pm, \tilde{\chi}_2^0} = 250$ GeV (black with filled area) in the heavy slepton scenario, and the SM background of the $j e^- \nu \nu$ (red) and $j e^- l \nu$ (blue) processes after applying the pre-selection cuts.

FCC-eh [1 ab ⁻¹]	Signal	Background	
$m_{\tilde{\chi}}$ [GeV]	250	$j e^- \nu \nu$	$j e^- l \nu$
$m_{\tilde{l}}$ [GeV]	-		
initial	909	1.08×10^6	7.96×10^6
Pre-selection	399	3.87×10^5	5.71×10^5
BDT > 0.1717	13.9	326	357
$\sigma_{\text{stat+sys}}$	0.32		

TABLE III. Cut-flow table for signal $j e^- \tilde{\chi} \tilde{\chi}$ with $M_{\tilde{\chi}_1^\pm, \tilde{\chi}_2^0} = 250$ GeV in the heavy slepton scenario, and the SM background processes $j e^- \nu \nu$ and $j e^- l \nu$. The numbers correspond to an integrated luminosity of 1 ab⁻¹ at the FCC-eh with unpolarized electron beam. The significance including 5% systematic uncertainty on the background are presented in the last row.

masses of $\tilde{\chi}_1^\pm$ and $\tilde{\chi}_2^0$ for the heavy slepton scenario at the FCC-eh with unpolarized beams and integrated luminosities of 1 ab⁻¹ and 2.5 ab⁻¹. For dashed (solid) curve, a systematic uncertainty of 0% (5%) on the background is included. When considering 0% (5%) systematic uncertainty on the background, the 2- σ limits on the $\tilde{\chi}_1^\pm$ and $\tilde{\chi}_2^0$ masses are 200 (125) GeV for 1 ab⁻¹ lumi-

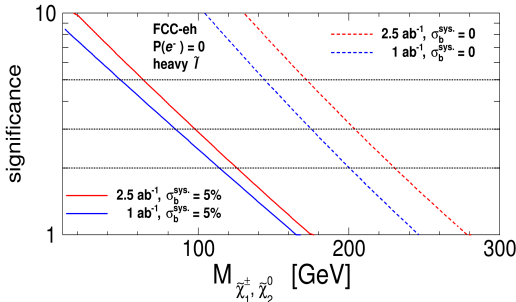


FIG. 7. Significances as varying the masses of $\tilde{\chi}_1^\pm$ and $\tilde{\chi}_2^0$ for the heavy slepton scenario at the FCC-eh with unpolarized beams and integrated luminosities of 1 ab⁻¹ and 2.5 ab⁻¹. For dashed (solid) curve, a systematic uncertainty of 0% (5%) on the background is considered.

osity, and 230 (114) GeV for 2.5 ab⁻¹ luminosity, respectively. When considering 0% systematic uncertainty on the background, the 5- σ limits are 144 GeV for 1 ab⁻¹ luminosity, and 172 GeV for 2.5 ab⁻¹ luminosity, respectively. Because of the small signal production, the discovery power for the heavy slepton scenario is limited at the future ep colliders.

V. CONCLUSIONS

The current LHC experiments have produced impressive constraints on the masses of coloured sparticle (gluinos and squarks). Due to the much lower direct production cross sections for the electroweakinos (neutralinos, charginos and sleptons), the current LHC constraints on electroweakino masses are limited, particularly in the compressed scenarios where the soft decay products also challenge the experimental analysis. In this article, we develop a search strategy for the SUSY dark matter and sleptons and forecast their discovery potential at the future electron-proton colliders, LHeC and FCC-eh. Our study reveals that the searches for the SUSY electroweakinos at the ep colliders could be complementary to the analyses at the pp colliders.

We focus on the compressed scenarios where the LSP $\tilde{\chi}_1^0$ is bino, $\tilde{\chi}_1^\pm$ and $\tilde{\chi}_2^0$ are wino with almost degenerate masses, and mass difference between $\tilde{\chi}_1^0$ and $\tilde{\chi}_1^\pm$ is 1 GeV. The signal is produced via the process “ $p e^- \rightarrow j e^- \tilde{\chi} \tilde{\chi}$ ”, where $\tilde{\chi} = \tilde{\chi}_1^0, \tilde{\chi}_1^\pm$ or $\tilde{\chi}_2^0$, and the final state has one jet, one electron, large missing energy and undetected very soft particles from $\tilde{\chi}_1^\pm$ or $\tilde{\chi}_2^0$ decays. The standard model background consists of the process with production of two neutrinos “ $p e^- \rightarrow j e^- \nu \nu$ ” and one neutrino “ $p e^- \rightarrow j e^- l \nu$ ”, where all flavors of leptons e, ν, τ are included. The kinematical observables are input to the TMVA package to perform the multivariate analysis at the detector level.

In the light slepton scenario, we consider the left-handed slepton \tilde{l} and sneutrino $\tilde{\nu}$ are slightly heavier than $\tilde{\chi}_1^\pm$ or $\tilde{\chi}_2^0$. When fixing mass difference $\Delta M = M_{\tilde{l}} - M_{\tilde{\chi}_1^\pm, \tilde{\chi}_2^0}$ to be 35 GeV and ignoring the systematic uncertainty on the background, our analysis indicates that the 2 (5)- σ limits on the $\tilde{\chi}_1^\pm, \tilde{\chi}_2^0$ mass are 616 (517) GeV for 2.5 ab⁻¹ luminosity at the FCC-eh, and 266 (227) GeV for 1 ab⁻¹ luminosity at the LHeC, respectively. To investigate the effects when varying ΔM , we fix $M_{\tilde{\chi}_1^\pm, \tilde{\chi}_2^0}$ to be 400 GeV and find that at the FCC-eh the significance is maximal when ΔM is around 20 GeV. In the heavy slepton scenarios where only $\tilde{\chi}_1^0, \tilde{\chi}_1^\pm$ and $\tilde{\chi}_2^0$ are light and other SUSY particles are heavy and decoupled, when neglecting the systematic uncertainty on the background, the 2 (5)- σ limits on the $\tilde{\chi}_1^\pm, \tilde{\chi}_2^0$ mass are 230 (172) GeV for 2.5 ab⁻¹ luminosity at the FCC-eh.

We find that 5% systematic uncertainty on the background can affect the limits greatly. Therefore, in order to enhance the discovery power of SUSY electroweakinos

at the future ep colliders, the controlling of the systematic uncertainty is very important.

Finally, we want to comment on the effects of the electron beam polarizations. At the ep colliders, the polarized electron beam is feasible. To investigate the effects of the electron beam polarizations on the discovery limits, we apply an electron beam polarization of -80% (+80%) at the FCC-eh and find that the production cross sections for the 2-neutrino background process $je^- \nu\nu$ and 1-neutrino background process $je^- l\nu$ can be increased (decreased) by a factor of about 55% and 20%, respectively. For the signal productions, in the light slepton scenario with $M_{\tilde{\chi}_1^\pm, \tilde{\chi}_2^0} = 400$ GeV and $M_{\tilde{l}} = 435$ GeV, at the FCC-eh the signal production cross section is increased (decreased) by a factor of about 80% corresponding to -80% (+80%) electron beam polarization, while in the heavy slepton scenario with $M_{\tilde{\chi}_1^\pm, \tilde{\chi}_2^0} = 250$ GeV and decoupled sleptons, the factor is about 40%. Therefore, due to much larger signal productions, the -80% electron beam polarization could possess stronger discovery potential for the SUSY electroweakinos especially for the light slepton scenario. At the FCC-eh with 1 ab^{-1} luminosity, for the light slepton scenario with benchmark mass $M_{\tilde{\chi}_1^\pm, \tilde{\chi}_2^0} = 400$ GeV and $M_{\tilde{l}} = 435$ GeV, our analysis indicates that compared with the unpolarized electron beam, the -80% electron beam polarization increases the significances from 9.28 to 12.89, and from 3.28 to 3.75 when including 0% and 5% systematic uncertainty on the background, respectively. For the heavy slepton scenario with benchmark mass $M_{\tilde{\chi}_1^\pm, \tilde{\chi}_2^0} = 250$ GeV, the -80% electron beam polarization increases the significances from 0.95 to 1.25, and from 0.32 to 0.35 when including 0% and 5% systematic uncertainty on the background, respectively. However, the limits with polarized electron beam polarization necessitate the simulation of the background and signal processes and re-doing the analysis for all mass points, which is beyond the scope of this study and we leave for future studies.

ACKNOWLEDGMENTS

We thank **** for the helpful communications. We appreciate the comments from other members in the LHeC / FCC-eh Higgs and BSM physics study groups. K.W. also wants to thank Christophe Grojean and Cai-dian Lü for helpful discussions and their supports. K.W. is supported by the International Postdoctoral Exchange Fellowship Program (No.90 Document of OCPC, 2015); G.A. by National Science and Engineering Research Council (Canada).

Appendix A: Distributions of Input Observables

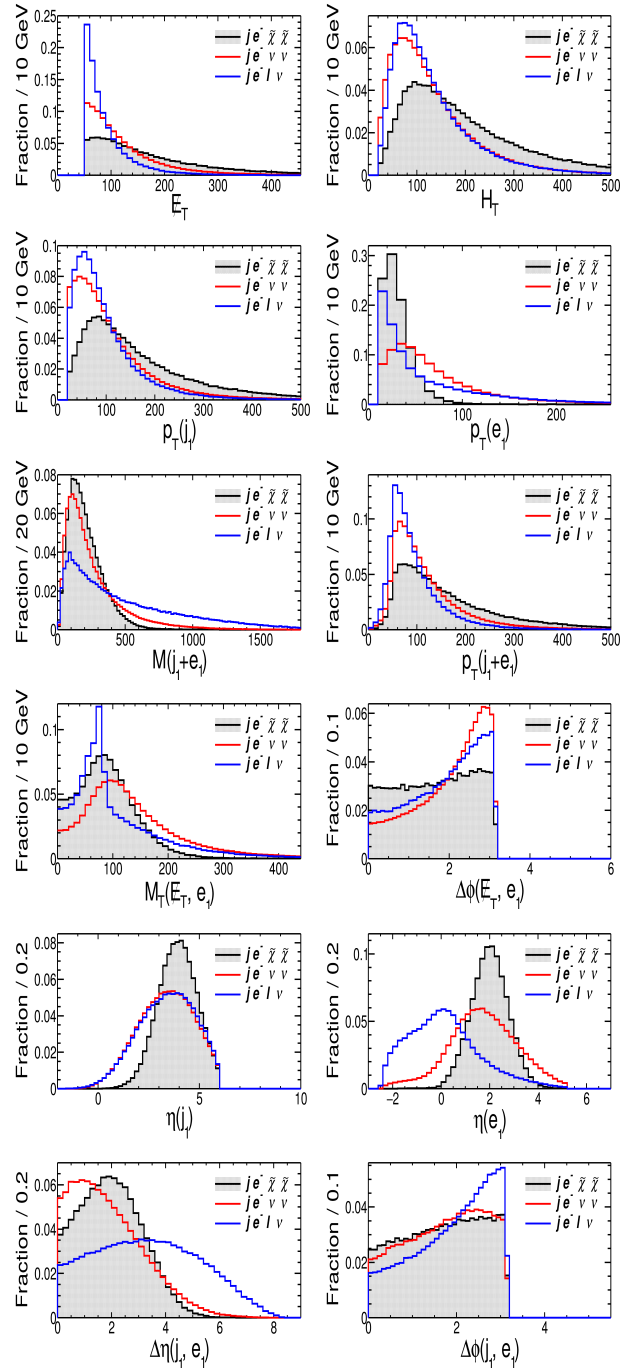


FIG. 8. Kinematical distributions of some input observables for signal $je^- \tilde{\chi}\tilde{\chi}$ with $M_{\tilde{\chi}_1^\pm, \tilde{\chi}_2^0} = 400$ GeV (black with filled area) in the light slepton scenario, and the SM backgrounds of the $je^- \nu\nu$ (red) and $je^- l\nu$ (blue) processes after applying the pre-selection cuts at the FCC-eh.

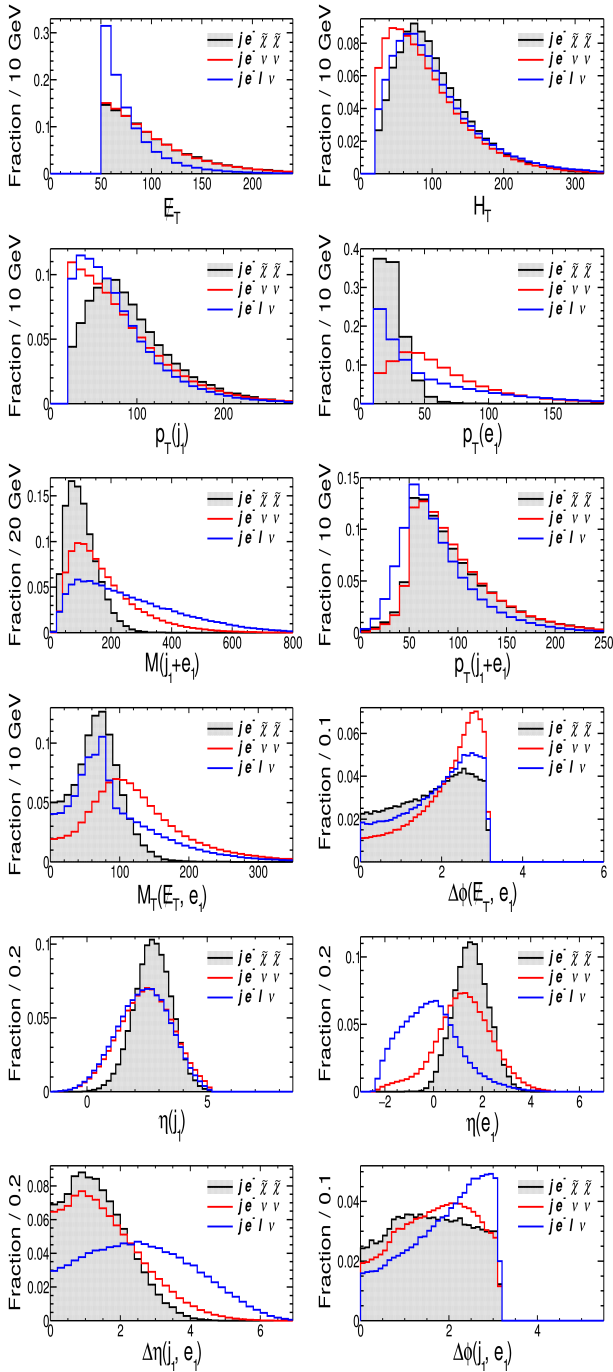


FIG. 9. Kinematical distributions of some input observables for signal $j e^- \tilde{\chi} \tilde{\chi}$ with $M_{\tilde{\chi}_1^\pm, \tilde{\chi}_2^0} = 250$ GeV (black with filled area) in the light slepton scenario, and the SM backgrounds of the $j e^- \nu \nu$ (red) and $j e^- l \nu$ (blue) processes after applying the pre-selection cuts at the LHC.

.....

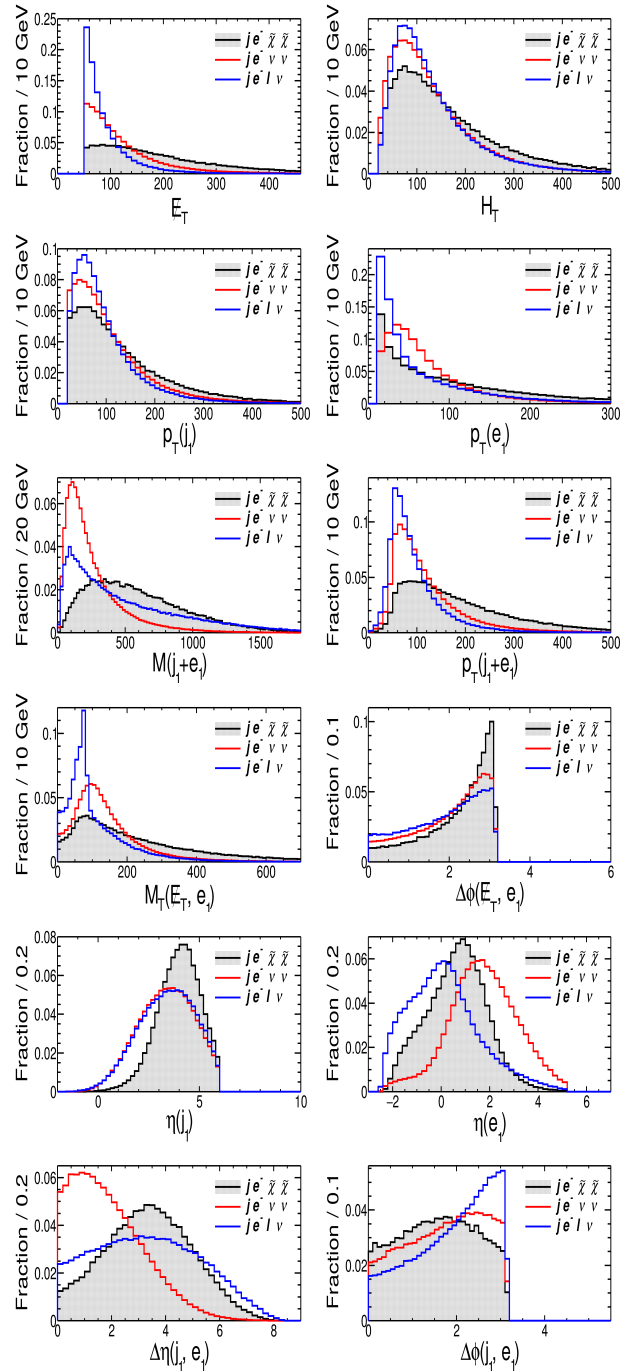


FIG. 10. Kinematical distributions of some selected input observables at the FCC-eh for signal $j e^- \tilde{\chi} \tilde{\chi}$ with $M_{\tilde{\chi}_1^\pm, \tilde{\chi}_2^0} = 250$ GeV (black with filled area) in the heavy slepton scenario, and the SM background of the $j e^- \nu \nu$ (red) and $j e^- l \nu$ (blue) processes after applying the pre-selection cuts.

.....

[1] M. Aaboud *et al.* [ATLAS Collaboration], arXiv:1712.02332 [hep-ex].

[2] A. M. Sirunyan *et al.* [CMS Collaboration],

- Phys. Rev. D **96**, no. 3, 032003 (2017) doi:10.1103/PhysRevD.96.032003 [arXiv:1704.07781 [hep-ex]].
- [3] A. M. Sirunyan *et al.* [CMS Collaboration], Eur. Phys. J. C **77**, no. 10, 710 (2017) doi:10.1140/epjc/s10052-017-5267-x [arXiv:1705.04650 [hep-ex]].
- [4] A. M. Sirunyan *et al.* [CMS Collaboration], JHEP **1803**, 160 (2018) doi:10.1007/JHEP03(2018)160 [arXiv:1801.03957 [hep-ex]].
- [5] G. Aad *et al.* [ATLAS Collaboration], JHEP **1405**, 071 (2014) doi:10.1007/JHEP05(2014)071 [arXiv:1403.5294 [hep-ex]].
- [6] G. Aad *et al.* [ATLAS Collaboration], JHEP **1404**, 169 (2014) doi:10.1007/JHEP04(2014)169 [arXiv:1402.7029 [hep-ex]].
- [7] G. Aad *et al.* [ATLAS Collaboration], Phys. Rev. D **93**, no. 5, 052002 (2016) doi:10.1103/PhysRevD.93.052002 [arXiv:1509.07152 [hep-ex]].
- [8] S. Chatrchyan *et al.* [CMS Collaboration], JHEP **1211**, 147 (2012) doi:10.1007/JHEP11(2012)147 [arXiv:1209.6620 [hep-ex]].
- [9] V. Khachatryan *et al.* [CMS Collaboration], Phys. Rev. D **90**, no. 9, 092007 (2014) doi:10.1103/PhysRevD.90.092007 [arXiv:1409.3168 [hep-ex]].
- [10] V. Khachatryan *et al.* [CMS Collaboration], Eur. Phys. J. C **74**, no. 9, 3036 (2014) doi:10.1140/epjc/s10052-014-3036-7 [arXiv:1405.7570 [hep-ex]].
- [11] A. M. Sirunyan *et al.* [CMS Collaboration], JHEP **1803**, 166 (2018) doi:10.1007/JHEP03(2018)166 [arXiv:1709.05406 [hep-ex]].
- [12] A. M. Sirunyan *et al.* [CMS Collaboration], arXiv:1801.01846 [hep-ex].
- [13] M. Aaboud *et al.* [ATLAS Collaboration], arXiv:1803.02762 [hep-ex].
- [14] Z. Han, G. D. Kribs, A. Martin and A. Menon, Phys. Rev. D **89**, no. 7, 075007 (2014) doi:10.1103/PhysRevD.89.075007 [arXiv:1401.1235 [hep-ph]].
- [15] H. Baer, A. Mustafayev and X. Tata, Phys. Rev. D **90**, no. 11, 115007 (2014) doi:10.1103/PhysRevD.90.115007 [arXiv:1409.7058 [hep-ph]].
- [16] G. F. Giudice, T. Han, K. Wang and L. T. Wang, Phys. Rev. D **81**, 115011 (2010) doi:10.1103/PhysRevD.81.115011 [arXiv:1004.4902 [hep-ph]].
- [17] A. G. Delannoy *et al.*, Phys. Rev. Lett. **111**, 061801 (2013) doi:10.1103/PhysRevLett.111.061801 [arXiv:1304.7779 [hep-ph]].
- [18] A. G. Delannoy *et al.*, arXiv:1308.0355 [hep-ph].
- [19] P. Schwaller and J. Zurita, JHEP **1403**, 060 (2014) doi:10.1007/JHEP03(2014)060 [arXiv:1312.7350 [hep-ph]].
- [20] S. Gori, S. Jung and L. T. Wang, JHEP **1310**, 191 (2013) doi:10.1007/JHEP10(2013)191 [arXiv:1307.5952 [hep-ph]].
- [21] B. Dutta *et al.*, Phys. Rev. D **91**, no. 5, 055025 (2015) doi:10.1103/PhysRevD.91.055025 [arXiv:1411.6043 [hep-ph]].
- [22] Z. Han and Y. Liu, Phys. Rev. D **92**, no. 1, 015010 (2015) doi:10.1103/PhysRevD.92.015010 [arXiv:1412.0618 [hep-ph]].
- [23] A. Barr and J. Scoville, JHEP **1504**, 147 (2015) doi:10.1007/JHEP04(2015)147 [arXiv:1501.02511 [hep-ph]].
- [24] M. Aaboud *et al.* [ATLAS Collaboration], Phys. Rev. D **97**, no. 5, 052010 (2018) doi:10.1103/PhysRevD.97.052010 [arXiv:1712.08119 [hep-ex]].
- [25] V. Khachatryan *et al.* [CMS Collaboration], Phys. Lett. B **759**, 9 (2016) doi:10.1016/j.physletb.2016.05.033 [arXiv:1512.08002 [hep-ex]].
- [26] K. Griest and D. Seckel, Phys. Rev. D **43**, 3191 (1991) doi:10.1103/PhysRevD.43.3191
- [27] J. Edsjo and P. Gondolo, Phys. Rev. D **56**, 1879 (1997) doi:10.1103/PhysRevD.56.1879 [hep-ph/9704361].
- [28] C. Han, R. Li, R. Q. Pan and K. Wang, arXiv:1802.03679 [hep-ph].
- [29] C. Patrignani *et al.* [Particle Data Group], Chin. Phys. C **40**, no. 10, 100001 (2016). doi:10.1088/1674-1137/40/10/100001
- [30] M. Endo, K. Hamaguchi, S. Iwamoto and T. Yoshinaga, JHEP **1401**, 123 (2014) doi:10.1007/JHEP01(2014)123 [arXiv:1303.4256 [hep-ph]].
- [31] LHeC Study Group, *A Large Hadron Electron Collider at CERN: Report on the Physics and Design Concepts for Machine and Detector*, J. Phys. G **39**, 075001 (2012)
- [32] M. Klein, arXiv:1802.04317 [hep-ph].
- [33] O. Brüning *et al.*, *Future Circular Collider Study FCC-he Baseline Parameters*, <https://fcc.web.cern.ch/Documents/FCCheBaselineParameters.pdf>
- [34] M. Klein, *LHeC Detector Design*, 25th International Workshop on Deep Inelastic Scattering, 2017, Birmingham, <https://indico.cern.ch/event/568360/contributions/2523637/>
- [35] Private communications with Max Klein, Uta Klein, Peter Kostka and Satoshi Kawaguchi.
- [36] J. Alwall *et al.*, *The automated computation of tree-level and next-to-leading order differential cross sections, and their matching to parton shower simulations*, JHEP **07** (2014) 79
- [37] T. Sjostrand, S. Mrenna and P. Skands, *A brief Introduction to PYTHIA8.1*, Comput. Phys. Commun. **178** (2008) 852
- [38] J. de Favereau *et al.* [DELPHES 3 Collaboration], *DELPHES 3, A modular framework for fast simulation of a generic collider experiment*, JHEP **1402** (2014) 057
- [39] A. Djouadi, M. M. Muhlleitner and M. Spira, Acta Phys. Polon. B **38**, 635 (2007) [hep-ph/0609292].
- [40] A. Hoecker, P. Speckmayer, J. Stelzer, J. Therhaag, E. von Toerne, and H. Voss, "TMVA: Toolkit for Multivariate Data Analysis," PoS A CAT 040 (2007) [physics/0703039].